J|A|C|S
ARTICLES
Published on Web 12/01/2006

Surface Tension and Fluid Flow Driven Self-Assembly of Ordered ZnO Nanorod Films for High-Performance Field Effect Transistors

Baoquan Sun* and Henning Sirringhaus

Contribution from Cavendish Laboratory, University of Cambridge, JJ Thomson Avenue, Cambridge, CB3 0HE United Kingdom

Received July 21, 2006; E-mail: bs309@cam.ac.uk

Abstract: Colloidal nanorods of inorganic semiconductors are of interest for a range of optoelectronic devices. The ability to self-assemble these materials into ordered arrays by solution-processing techniques is crucial for achieving adequate device performance. Here we show that uniform ZnO nanorod films with defined nanorod alignment can be solution-deposited over large areas by controlling the surface energy of the nanorods through the choice of suitable ligands and by the fluid flow direction during growth. ZnO nanorods with long carbon chain ligands exhibit a smaller surface free energy than those with short carbon chain ligands resulting in better in-plane alignment and large domain sizes up to dozens of micrometers in spin-coated films. A model is presented to rationalize the observed self-assembly behavior. It is based on the formation of a lyotropic liquid crystalline phase on the surface of the liquid film which is facilitated by enhanced segregation of nanorods with low surface tension to the surface. Alignment of the nanorods is controlled by radial and vertical liquid flows in the drying solution. The ability to control the orientation of the nanorods and to achieve large domain size results in significant device performance improvement. Field-effect transistors with mobilities of up to 1.2−1.4 $cm^2/V{\cdot}s$ are demonstrated in spin-coated, in-plane aligned ZnO nanorod films subject to postdeposition hydrothermal growth.

Introduction

The ability to assemble functional one-dimensional (1D) nanoscale materials such as nanotubes, nanowires, and nanorods into mesoscale ordered structures is a crucial prerequisite for their application in optoelectronic devices. It has been shown that uniaxial alignment of long semiconducting nanowires can result in significant improvements of optoelectronic properties.[1] Techniques for alignment of these materials can be divided into two categories: the first one is based on using external forces such as flow in microchannels,[2] Langmuir−Blodgett deposition,[3] and electrical fields;[4] the other is using internal interactions to self-assemble the 1D objects into well-ordered structures.[5,6] The self-assembly of colloidal nanorods from solution is attracting increasing attention because of the ease of fabricating well-ordered structures.[7,8] On the basis of this technique, the manufacturing of solution-processed optoelectronic devices can be simplified by using spin-coating, drop-casting, and direct printing techniques. Recently, considerable progress has been made to prepare ordered structures by solution self-assembly of spherical metal nanoparticles,[9−11] semiconductor nanospheres,[12−14] and semiconductor nanorods.[5,15] However, less is known about how to use these well-ordered superlattice structures for optoelectronic applications.[16]

ZnO nanorods are an attractive model system to study the self-assembly process and the correlation with device performance because stable dispersions with concentrations of typically up to 50 mg/mL can be prepared using suitable ligands.[17] ZnO is also currently attracting a lot of attention for applications as a transparent semiconductor for a range of thin film electronic applications, although in most cases amorphous or nanocrystalline ZnO films deposited by sputtering are used.[18,19] Here,

(1) Duan, X. F.; Niu, C. M.; Sahi, V; Chen, J; Parce; J. W.; Empedocles, S.; Goldman, J. L. *Nature* **2003**, *425*, 274−278.
(2) Huang, Y.; Duan, X. F.; Wei, Q. Q.; Lieber, C. M. *Science* **2001**, *291*, 630−633.
(3) Kim, F.; Kwan, S.; Akana, J.; Yang, P. D. *J. Am. Chem. Soc.* **2001**, *123*, 4260−4361.
(4) Harnack, O.; Pacholski, C.; Weller, H.; Yasuda, A.; Wessels, J. M. *Nano Lett.* **2003**, *3*, 1097−1101.
(5) Li, L. S.; Alivisatos, A. P. *Adv. Mater.* **2003**, *15*, 408−411.
(6) Jana, N. R. *Angew. Chem. Int. Ed.* **2004**, *43*, 1536−1540.
(7) Pileni, M. P. *J. Phys. Chem. B* **2001**, *105*, 3358−3371.
(8) Collier, C. P.; Vossmeyer, T.; Heath, J. R. *Annu. Rev. Phys. Chem.* **1998**, *49*, 371−404.
(9) Bigioni, T. P.; Lin, X. M.; Nguyen, T. T.; Corwin, E. I.; Witten, T. A.; Jaeger, H. M. *Nat. Mater.* **2006**, *5*, 265−270.
(10) Fink, J.; Kiely, C. J.; Bethell, D.; Schiffrin, D. J. *Chem. Mater.* **1998**, *10*, 922−926.
(11) Kiely, C. J.; Fink, J.; Brust, M.; Bethell, D.; Schiffrin, D. J. *Nature* **1998**, *396*, 444−446.
(12) Urban. J. J.; Talapin, D. V.; Shevchenko, E. V.; Murray, C. B. *J. Am. Chem. Soc.* **2006**, *128*, 3248−3255.
(13) Murray, C. B.; Kagan, C. R.; Bawendi, M. G. *Annu. Rev. Mater. Sci.* **2000**, *30*, 545−610.
(14) Redl, F. X.; Cho, K. S.; Murray, C. B.; O'Brien, S. *Nature* **2003**, *423*, 968−971.
(15) Talapin, D. V.; Shevchenko, E. V.; Murray, C. B.; Kornowski, A.; Forster, S.; Weller, H. *J. Am. Chem. Soc.* **2004**, *126*, 12984−12988.
(16) Talapin, D. V.; Murray, C. B. *Science* **2005**, *310*, 86−89.
(17) Sun, B.; Sirringhaus, H. *Nano Lett.* **2005**, *5*, 2408−2413.
(18) Fortunato, E. M. C.; Barquinha, P. M. C.; Pimentel, A. C. M. B. G.; Goncalves, A. M. F.; Marques, A. J. S.; Pereira, L. M. N.; Martins, R. F. P. *Adv. Mater.* **2005**, *17*,590−594.
(19) Carcia, P. F.; McLean, R. S.; Reilly, M. H.; Nunes, G. *Appl. Phys. Lett.* **2003**, *82*, 1117−1119.

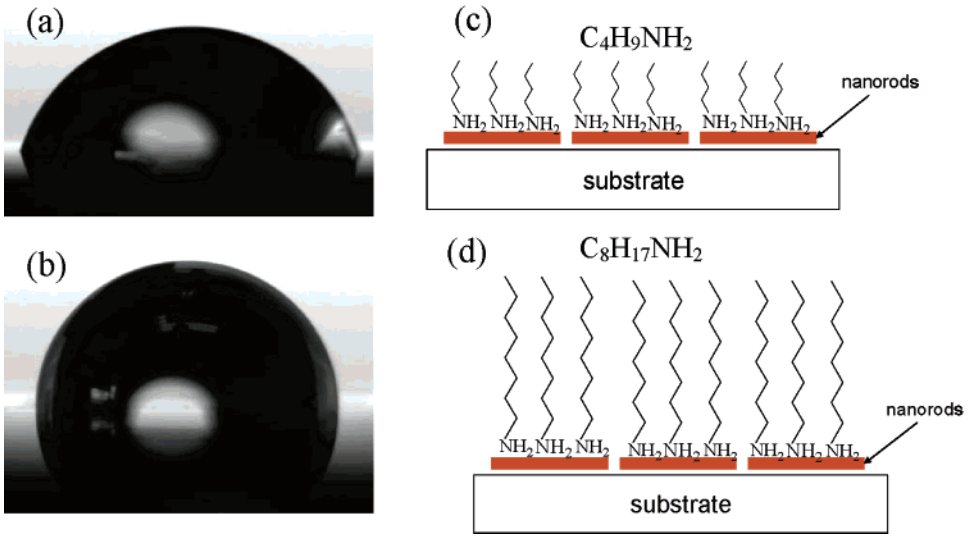

Figure 1. Photographs of water droplets on the surface of (a) spin-coated BUTA-ZnO film and (b) OCTA-ZnO film. The right cartoon images show their responding nanorod surface ligands (c) butylamine and (d) octylamine.

we investigate the dependence of the solution self-assembly of semiconducting ZnO nanorods on the length of the alkylamine ligand attached to the surface of the nanorods. We also study how the assembly properties are affected by the method of film deposition, in particular, by the direction of fluid flow during the growth of the film. We evaluate the electrical performance of self-assembled films of ZnO nanorods as the active semiconducting layer of field-effect transistors (FETs) as a function of the ligand length.

Experimental Procedures

Preparation of ZnO nanorods follows our previously reported method.[17] Zinc acetate and a small amount of water was added into methanol and heated to 60 °C with magnetic stirring. Potassium hydroxide in methanol was dropped into zinc acetate solution and heated for 2 h and 15 min. At this time, the solution was white and cloudy. The solution was cooled to room temperature, and nitrogen purging was used to condense the solvent. The solution became clear again when the solution volume was decreased to a certain volume. It was then reheated for another 5 h to obtain ZnO nanorods. The nanorods were washed twice using methanol. The nanorod average diameter was 11 nm, and the length was 92 nm determined by transmission electron microscopy (TEM) using a Philips Tecnai20 instrument. Finally, the ligands were attached to the surface, and the nanorods were dispersed in chloroform/methanol with a concentration of up to 50 mg/mL. It is very important to keep an accurate ratio between zinc acetate and potassium hydroxide for the nanorods to be well dispersed. Accurate stoichiometry is also critical to control the conductivity of the ZnO nanorod film.[17] FET devices were fabricated in standard bottom-gate, top-contact configuration. Nanorod solutions with approximate concentration of 25 mg/mL were spin-coated on a SiO_2 (300 nm)/Si substrate modified with hexamethyldisilazane (HMDS). The doped silicon wafer acts as the gate electrode. After the samples were annealed at 230 °C in forming gas N_2/H_2 (V/V, 95:5) for 30 min, a 100-nm-thick aluminum layer was evaporated through a shadow mask for the source and drain contacts. Scanning electron microscopy (SEM) and polarized optical microscopy (POM) imaging were performed directly on the active layer of the device substrates. SEM images were taken using a Philips XL30 electron microscope with an accelerating voltage of 15 kV. All the samples had been mildly annealed to reduce charging effects before being put into the SEM chamber. The sessile contact angles were measured for a drop of water on spin-coated ZnO films. The surface tension values of all the solvents including pure chloroform, pure methanol, mixed chloroform/methanol, and mixed chloroform/methanol/alkylamine were determined by a Kruss Process Tensiometer K12 using the ring method.

Results and Discussion

Effect of Ligand on Surface and Interface Tension. To keep the nanorods well dispersed in an organic solvent, an organic monolayer ligand is attached to the surface of the inorganic nanorod. For ZnO nanorods, acetate groups can be used during the initial synthesis of the nanorods. However, acetate groups have a short chain length and can result in the nanorods being negatively charged. To make the nanorods disperse in other organic solvents, butylamine (BUTA) was used as ligand in our previous report. BUTA is attached on the ZnO surface by an interaction between the nitrogen atom of BUTA and the zinc atom of ZnO. An attractive feature of this ligand is that it can be removed easily by low temperature annealing due to its neutral charge property and low boiling point. This is important for achieving efficient charge transport between the nanorods. In the present work, we used systematically alkylamine ligands with different chain lengths to tune the surface chemistry of the ZnO nanorods and to study the effect of the different ligand lengths on the self-assembly properties of the nanorods.

We found that the use of different ligand lengths results in a significant variation of the surface tension. A higher water contact angle is observed for water droplets deposited on nanorod films with longer carbon ligands. As shown in Figure 1 for octylamine (OCTA)-modified ZnO films, a water contact angle of 85.0° is observed compared to 74.4° (water) for BUTA-ZnO films. The contact angle θ is related to the particle−air surface tension $\gamma_{p/a}$, the liquid−air surface tension $\gamma_{l/a}$, and the liquid−particle interface $\gamma_{l/p}$ tension through Young's equation $\gamma_{p/a} = \gamma_{l/a} \cos \theta + \gamma_{l/p}$. In this case, the liquid is water. These contact angle measurements suggest that BUTA-ZnO particles might have a higher surface tension than OCTA-ZnO ones. However, to estimate quantitatively the surface tensions from the measured contact angles, the interfacial tensions need to be known, and we have used a simple theoretical model to estimate these which is presented as Supporting Information. From this

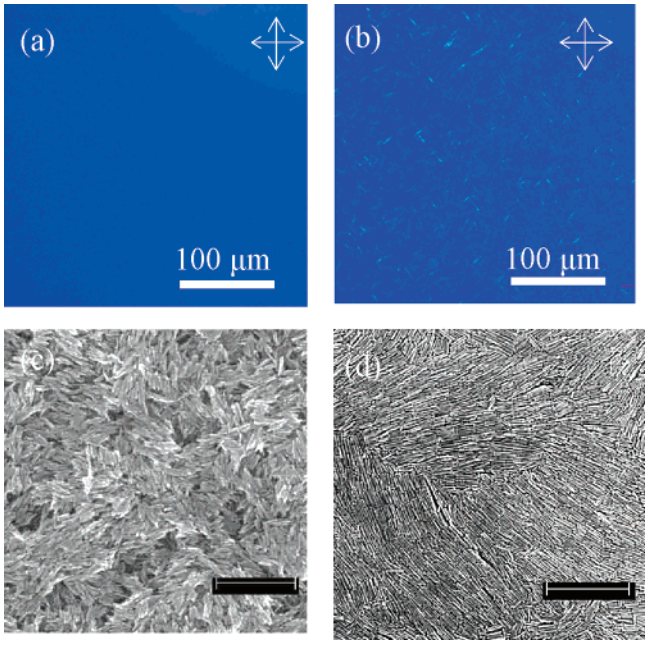

Figure 2. POM images of (a) butylamine-ZnO and (b) octylamine-ZnO films prepared by spin-coating. Images (c) and (d) are top view SEM image of spin-coated ZnO films with (c) butylamine (d) octylamine ligand. The length of the scale bars in (c) and (d) is 500 nm.

model, we estimate the difference between the surface tension of BUTA-ZnO ($\gamma_{p/a}^{BUTA} = 33.94$ mJ/m^2) and that of OCTA-ZnO ($\gamma_{p/a}^{OCTA} = 27.78$ mJ/m^2) to be 6.16 mJ/m^2. This needs to be compared to the surface energy $\gamma_{l/a}$ of the chloroform/methanol solvent (3/1, v/v) used for the film deposition which was determined experimentally by the ring method to be 26.74 mJ/m^2. This is in between the methanol surface energy $\gamma_{methanol/air} = 22.98$ mJ/m^2, and the chloroform surface energy $\gamma_{chloroform/air} = 28.02$ mJ/m^2.[20] We will use these values below to assess the ability of the nanorods to self-assemble at the liquid−air interface.

Effect of Ligand and Film Deposition on Nanorod Self-Assembly. We investigated the nanorod solution self-assembly for different film deposition techniques as a function of ligand length and compared in particular spin-coating and drop-casting. ZnO nanorods with alkylamine ligands can be well dispersed in chloroform/methanol solvent with high concentration (up to 50 mg/mL) enabling formation of uniform thin films by spin-coating. When solutions of ZnO nanorods with different ligand lengths are spin-coated on the substrate, the resulting films exhibit a strong variation of microstructure depending on the length of the ligand. In OCTA-ZnO films with low surface free energy clear optical contrast is observed in POM images with crossed polarizers indicating the presence of large crystalline domains with uniaxial alignment of the nanorods on a length scale of several 1−10 μm (Figure 2b). In contrast in BUTA-ZnO films, the crossed-polarizer images are uniformly black suggesting that the film is more optically isotropic, i.e., that crystalline order in the film is either absent or occurs on a submicrometer length scale that is too short to be observable by POM (Figure 2a). In hexylamine (HEXA)-modified ZnO

(20) We note that we have not been able to observe surfactant action of the alkylamine molecule in the chloroform/methanol solvent, i.e., no lowering of the solvent surface tension compared to that of the pure solvent was observed when alkylamine molecules were dissolved at a concentration of 1.5%, v/v in chloroform/methanol.

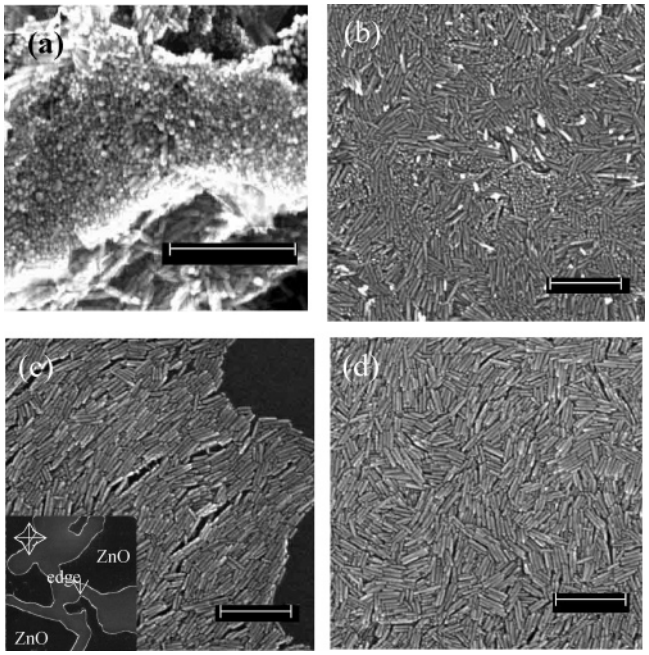

Figure 3. Top view of SEM images of OCTA-ZnO film on silicon oxide/silicon substrate processed under different conditions. (a) Nanorod film fabricated by drop-casting with slow (a) and high (b) evaporation rate. (c) Nanorod film dried between a glass and a Si/SiO_2 wafer showing the edge of the film (c) and the interior of the same film away from the edge (d). The inset in (c) shows a large-area POM image of this film. The length of the scale bars in (a−d) is 200 nm. The size of the image in the inset of (c) is 480 × 480 μm.

intermediate behavior with optical contrast somewhat weaker and occurring on a shorter length scale than in films of OCTA-ZnO was observed (not shown).

The origin of the optical contrast in the POM image was investigated by SEM. In all spin-coated films, we observed preferential in-plane alignment of the long-axis of the nanorods (Figure 2c,d). However, in the OCTA-ZnO films, large domains are present in which the nanorods are aligned uniaxially parallel to each other in the plane of the film. Only a few domain boundaries are visible in the SEM image of Figure 2d. In contrast, in the BUTA-ZnO case (Figure 2c), although the nanorods are also aligned preferentially in the plane of the film, only much smaller domains are present, and over a length scale of 1 μm the orientation of the nanorods appears isotropic. The SEM observations explain the optical contrast observed in POM and show clearly that the ligand length has an important influence on the ability of the nanorods to form large-scale uniaxially oriented microstructures.

Different behavior was observed in the case of drop-casting. When a droplet of nanorod OCTA-ZnO solution was dried on the substrate with a slow evaporation rate, we observed preferential out-of-plane alignment of the nanorods in contrast to the in-plane alignment observed in spin-coated films. In some areas, well-defined uniaxial ordering was observed that manifests itself in well-defined steps on the surface of the film (Figure 3a. When the films were drop-cast under fast evaporation conditions, a more disordered structure with more random orientation of the nanorods resulted (Figure 3b). A similar structure has been reported recently for CdSe crystalline nanorod solids,[15] which were prepared by allowing nanorods to assemble slowly at the liquid−liquid interface on carbon-coated copper grids. CdSe nanorods with *n*-octadecylphosphonic acid ligands

can self-organize into nematic and smectic structures by slow destabilization of a nanorod solution upon allowing the diffusion of a non-solvent into the colloidal solution.

We also investigated the drying of a drop of nanorod solution in between two substrates (bottom SiO_2/Si wafer and top quartz substrate), such that the free solution−air interface was not present, and evaporation occurred at the edges of the liquid film stacked between the two substrates. Under such conditions, a well-ordered nanorod structure can be observed where nanorods are again oriented parallel to the substrate as in spin-coated films. In the vicinity of the edges of the film, the nanorods are aligned uniaxially perpendicular to the contact line as shown in Figure 3c. This well-ordered assembly takes place at the edge of the drying solution where solvent evaporation leads to a liquid flow in the plane of the film perpendicular to the contact line. POM images of a drop of OCTA-ZnO nanorods dried between the two substrates show bright contrast at the edges of the film reflecting this uniaxial alignment of the nanorods (see inset of Figure 3c). The films made in this way are not continuous though. In areas of the films that are more than a few micrometers away from the contact line in-plane nanorod alignment without uniaxial alignment along a preferred direction is observed (Figure 3d).

By comparing substrates with and without surface treatment using self-assembled monolayers, such as HMDS, we found that the orientation and assembly of the nanorods is not sensitive to the substrate surface tension. These observations suggest that the liquid flow in the drying solution and the presence of the liquid−air interface play important roles in determining nanorod self-assembly.

Model for Solution Self-Assembly. To understand nanorod assembly for the different deposition conditions, we use a model that has recently been proposed to explain the nucleation and growth of colloidal crystal monolayers of metallic nanoparticles at the solution−air interface.[9] The fluid dynamics of the spin-coating process is very complex, and therefore we consider first the much simpler situations of drop-casting at a low evaporation rate and drying between two substrates to identify the key fluid dynamical factors that determine nanorod alignment. In the case of drop-casting due to evaporation, solvent molecules move toward the interface from the interior to replenish the surface liquid and the surface moves toward the substrate. At the same time, nanorods diffuse in solution. Under the conditions used here, the diffusion velocity is slower than the velocity of the moving liquid−air interface,[9] and therefore nanorods from the interior of the solution are swept toward the surface. The flux of nanorods impinging onto the surface is given by $f = c\upsilon$, where c and υ are the concentration and flow rate of nanorods with respect to the surface, respectively. According to the Onsager-Flory rigid rod model[21] at sufficiently low concentration of the rods in solution, the rod orientation is isotropic. However, as the concentration increases, it becomes increasingly difficult for the rods to point in random directions, and a concentrated solution of nanorods will undergo a phase transition into a lyotropic liquid crystalline phase in which the nanorods are aligned uniaxially along a director. This phase transition is expected to occur at a critical volume ratio of nanocrystals to solvent of $\varphi_0 = cD/L$, where c is a constant with a value $c =$ 4.5 in the Onsager model. D is the rod diameter, and L is its length. For the rigid rod theory to be valid, a few criteria need to be fulfilled:[22] The only important forces between rods are assumed to be steric forces and the rods do not interpenetrate each other. The length of the nanorods needs to be significantly larger than their diameter ($L >> D$). In our case, L/D is approximately 8. For the purpose of this estimate, the effect of the ligand on the dimensions of the nanorods can be ignored. Therefore, the colloidal nanorod solution may satisfy the assumptions made by the rigid rod model.

To reach the critical concentration for the liquid−crystalline phase transition on the surface which is believed to promote a high degree of nanorod alignment, it is desirable to promote segregation and nucleation of the nanorods to the liquid−air interface. To explain the observed difference in self-assembly between OCTA- and BUTA-ZnO we postulate that as a result of its lower surface tension as suggested by the measured contact angle the OCTA-ZnO nanorods have a stronger tendency to segregate to the liquid−air interface than the BUTA-ZnO ones. The driving force for nanorod segregation to the surface can be estimated by calculating the difference of surface potential $\Delta\mu$ between a nanorod completely immersed in solution and a nanorod segregated to the surface and exposing a portion of its surface to air. In Supporting Information, we present a theoretical estimate of this change of surface potential based on the experimentally determined contact angles and surface tensions. The analysis shows indeed that as a result of a lower surface as well as higher interface tension in chloroform/methanol ($\gamma_{p/l}^{BUTA} = 0.670$ mJ/m^2 and $\gamma_{p/l}^{OCTA} = 1.21$ mJ/m^2) the OCTA-ZnO nanorods are expected to experience a favorable driving force to segregate to the surface, while for BUTA-ZnO it is energetically unfavorable to expose a portion of the nanorod surface at the liquid−air interface. The lowering of surface potential upon exposing the end of the nanorod on the surface is estimated to be $\Delta\mu_l^{BUTA} = -0.244\pi R^2\gamma_{l/a}$ in the case of BUTA-ZnO, and $\Delta\mu_l^{OCTA} = 0.063\pi R^2\gamma_{l/a}$ for OCTA-ZnO, where $\gamma_{l/a}$ is surface energy of chloroform/methanol, and R is the radius of the nanorod. Here the nanorod is assumed to be oriented with its long axis normal to the liquid−air interface, and exposing one of its end cross-sections to air.

A nanorod is considered to be trapped at the liquid−air interface if $\Delta\mu_l$ is positive, and the surface potential change $\Delta\mu_l$ is closely related to the diffusion length λ of the nanorods on the surface $\lambda^2 = 2L^2 \exp[\Delta\mu_l/k_bT]$ where k_b and T are Boltzmann's constant and temperature.[9] For the above values of $\Delta\mu_l$, this relationship shows that small changes of surface potential change due to differences in surface tension between different ligands can result in large differences of diffusion length, as shown in Scheme 1g. For the BUTA-ZnO, the surface potential change value is negative, which means the nanorods have to overcome a potential barrier from interior bulk liquid to interface. This barrier will prevent the nanorods from segregating toward the interface. In contrast, the estimated surface potential change $\Delta\mu_l^{OCTA}$ is positive, which means that a driving force exists that favors the nanorod segregation toward the air−liquid interface. Using the interfacial potential change $\Delta\mu_l^{oct} = 3.89k_bT$, we estimate the diffusion length λ^{OCTA} to be on the order of ∼0.91 μm. A long diffusion length is closely

(21) Chandrasekhar, S. *Liquid Crystals*, 2nd ed.; Cambridge University Press: Cambridge, 1992.

(22) Gennes, P. G.; Prost, J. *The Physics of Liquid Crystals*, 2nd ed.; Claredon Press: Oxford, 1993.

Scheme 1[a]

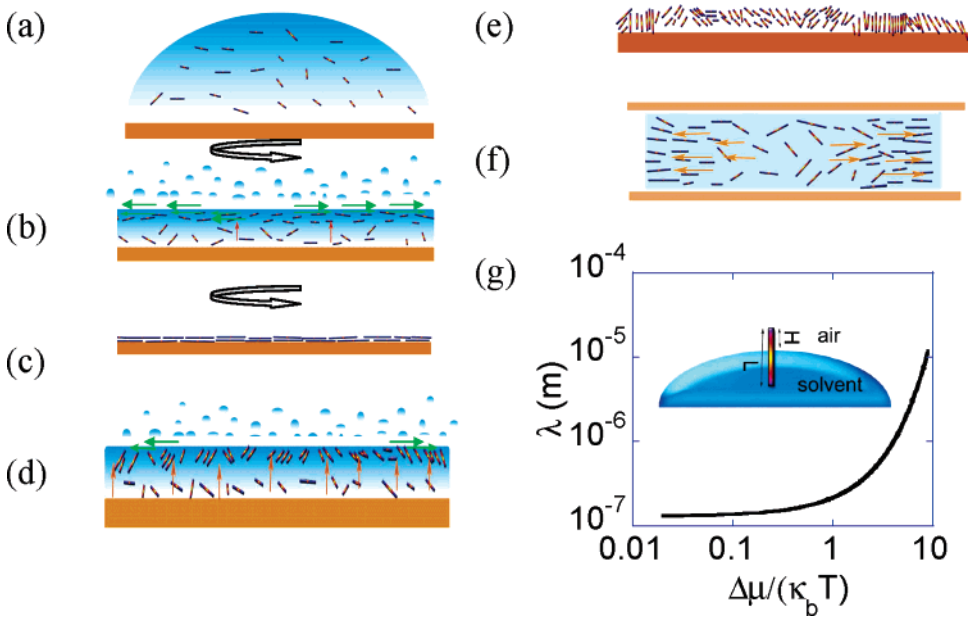

[a] Panels (a−c): A schematic diagram illustrating the different stages of spin-coating a solution of ZnO nanorods. Initially, nanorods are mono-dispersed in the whole drop of solution (a). When the substrate is rotating, the liquid film is thinned and due to evaporation the solute concentration on the surface is enhanced. (b) Nanorods can be aligned due to the radial fluid flow. The orange arrows indicate the upward solvent flow due to evaporation and replenishing of surface molecule. Green arrows indicate the radial flow due to the rotation of the substrate. When the solute concentration on the surface is high enough, the phase transition from isotropic to mesomorphic phase will happen (c). Panels (d) and (e) illustrate how those nanorods self-assemble during the process of in dropping casting. Under slow evaporation the process is dominated by vertical flow due to evaporation (d) leading to vertical alignment of the nanorods (e). (f) Shows schematically the situation for solution drying between two substrates. (g) The nanorod diffusion length on the surface is amplified exponentially by the surface potential difference between nanorods in the interior bulk solvent and at the liquid−air surface. The inset illustrates a nanorod of length L penetrating by a distance H above the surface of the liquid.

related to the critical concentration φ_0 for the liquid−crystalline phase transition. A certain minimum flow rate value f_0 is needed to reach this concentration, which can be estimated to be $f_0 = 4\varphi_0 D_{\text{diff}}/\lambda^2$, where D_{diff} is the diffusion constant at the liquid−air interface.[9] From this expression, it is clear that nanorods with longer diffusion length at the liquid−air interface are more likely to reach the critical concentration to undergo nucleation on the surface. This analysis suggests that the reason for the larger domain size of the OCTA-ZnO films is related to the ability of the OCTA-ZnO nanorods to undergo nucleation at the air−liquid interface. In the case of nanorods which do not have a tendency to segregate to the surface, such as BUTA-ZnO, it is more likely that nucleation occurs in the bulk of the liquid leading to poorer alignment of the nanorods.

Within this framework, once the lyotropic solution has formed on the drying surface the orientation of the nanorods is expected to be determined by flow alignment due to the solution flow on the surface. This explains why in the case of drop-casting the preferred orientation of the nanorods is perpendicular to the substrate since in this case the dominant solution flow is due to evaporation and is normal to the surface (Scheme 1d). In the case of the nanorod solution drying between two substrates (Scheme 1f), the nucleation is expected to occur at the edges of the drying film where solvent can escape between the two substrates and where the concentration is highest. Here the solution flow is in the plane perpendicular to the edge, and this explains the strong uniaxial alignment, and in some cases even smectic alignment of the rods near the edge of the film. This observation also supports the conclusion that under these conditions the transition from isotropic phase to lyotropic phase happens preferentially at the liquid−air interface where the concentration is highest and not in the bulk interior of the solution.

The case of drop-casting with high evaporation rate (Figure 3b) is more complex to explain. Here we observed a complex alignment motive with small domains that adopt either in-plane, out-of-plane, or tilted alignment of the nanorods. This might be related to a complex pattern of liquid flow on the surface. In this situation, one would expect to observe a normal component of the flow due to replenishment of solvent evaporating at the surface, a lateral flow along the substrate to transport liquid to the edges of the film that have a higher evaporation rate (coffee-stain effect).[23] It is also possible that convective flow cells might be formed driven by either a temperature gradient or a concentration gradient on the surface caused by the evaporation of solvent.[24] An alternative explanation for the nonuniform alignment under such process conditions is that nucleation occurs in the bulk of the solution at a stage when the film is still thick enough, such that capillary forces do not force in-plane alignment of the rod (see discussion below).

We now turn to a discussion of the much more complex situation in spin-coating. We assume that the fluid flow direction that has been shown clearly above to determine the alignment in the case of drop-casting and drying between two substrates is also critical in the more complex spin-coating process. The various factors that control deposition in the spin-coating process

(23) Deegan, R. D.; Bakajin, O.; Dupont, T. F.; Huber, G.; Nagel, S. R.; Witten, T. A. *Nature* **1997**, *389*, 827−829.
(24) Denkov, N. D.; Velev, O. D.; Kralchevsky, P. A.; Ivanov, I. B.;, Yoshimura, H.; Nagayama, K. *Langmuir* **1992**, *8*, 3183−3190.

have been extensively studied[25−29] and include the solution concentration, density, viscosity, surface free energy, solution evaporating rate, and rotation speed. When a film is fabricated by spin-casting from nanorod solution with high solvent drying rate, the liquid flow has both an in-plane component due to rotation of the substrate as well as an out-of-plane component due to evaporation at the surface. The spin-coating process can be divided into several stages.[28] In the early stages the process is determined by the radial convection flow due to the rotation of the substrate leading to initially rapid thinning of the film, while the solute concentration in the liquid remains constant. The radial flow velocity is highest on the surface and drops to zero at the interface with the solid substrate. As the film thins the radial flow velocity and the film thinning rate due to convection slow down, and evaporation of solvent at the surface begins to make an increasingly important contribution to the thinning of the film. In this stage, the solute concentration on the surface is expected to become larger than the concentration in the bulk. Finally, the radial flow comes almost to a halt, and solvent evaporation results in rapid increase of solute concentration in the film. Several factors might lead to preferential in-plane alignment of the nanorod solution in this process. If the nanorods have a strong tendency to segregate to the surface of the liquid film driven by their low surface tension in the case of OCTA-ZnO it is possible that the critical concentration for forming a lyotropic phase on the surface is reached at a stage when there is still a sufficiently high, in-plane radial flow velocity to align the nanorods in the plane (Scheme 1c). Ideally, in this situation one might expect a uniform radial alignment of the rods, which is clearly not observed (Figure 2). Such radial flow alignment might be present during spin-coating but is not preserved when the liquid crystalline phase solidifies and crystalline domains with random orientation of the nanorods nucleate. We postulate that the nucleation of crystalline domains might occur at a point at which the film has already thinned down to a thickness that is comparable or less than the length of the nanorods forcing the nanorods to retain their in-plane orientation. In this way, the orientation of the nanorods in the crystalline domains would be expected to be randomly oriented in the plane as observed experimentally. This model is also able to explain our observation that in more concentrated solutions (50 mg/mL) processed by spin-coating the nanorods are not aligned in the plane but adopt a tilted orientation with respect to the substrate. This might indicate that in concentrated solutions nucleation occurs at a stage when the liquid film thickness is still significantly larger than the length of the nanorods; however, further work is required to investigate the various factors that affect nanorod alignment in spin-coated films in more detail.

Thin Film Transistor Based on Self-Assembly ZnO Films. The ability to self-assemble the nanorods into well-aligned structures can be exploited to achieve significantly improved electrical transport in solution-processed ZnO films. Although there are several studies that report alignment of colloidal semiconductor nanorods, to the best of our knowledge there is only very few studies that investigate the correlation between nanorod alignment and charge carrier mobility. This is possibly because of a small, sub-micrometer domain size,[3,5,30] or difficulties of integrating the aligned films into device configurations.[15,31] Here we can control the alignment of the nanorods in spin-coated films that can easily be integrated into FET structures, and using ligands such as OCTA-ZnO it is possible to produce films with favorable in-plane alignment of the nanorods and domain size of several micrometers. Here we investigate the correlation between the field-effect transistor performance and the nanorod alignment in spin-coated ZnO films with different ligands.

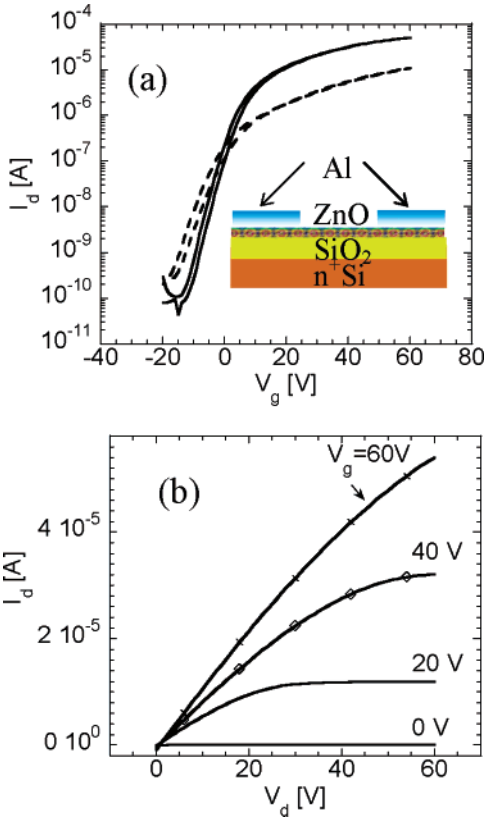

Figure 4. (a) Saturated (V_d = 60 V) transfer characteristics for as-made TFT fabricated by spin-coating of ZnO nanorods with different ligands, solid line (OCTA-ZnO), dashed line (BUTA-ZnO). (b) Output characteristics of a spin-coated device made from OCTA-ZnO nanorods. The TFT device structure is shown in the inset in (a).

FETs were fabricated in a standard bottom-gate, top-contact configuration using highly doped silicon wafers acting as gate electrodes with a 300-nm SiO_2 gate dielectric (Figure 4a). The SiO_2 surface was modified by a self-assembled monolayer of HMDS prior to spin-coating of the active ZnO nanorod film. The HMDS substrate modification was found to lead to better device performance compared to films deposited onto unmodified, hydrophilic SiO_2. HMDS and other self-assembled monolayers render the surface hydrophobic and are widely used in organic thin film transistors (TFTs).[32] We did not observe

(25) Bornside, D. E.; Macosko, C. W.; Scriven, L. E. *J. Appl. Phys.* **1989**, *66*, 5185−5193.
(26) Emslie, A. G.; Bonner, F. T.; Peck, L. G. *J. Appl. Phys.* **1958**, *29*, 858−862.
(27) Lawrence, C. J. *Phys. Fluids* **1988**, *31*, 2786−2795.
(28) Ohara, T.; Matsumoto, Y.; Ohashi, H. *Phys. Fluids A* **1989**, *1*, 1949−1959.
(29) Birnie, D. P. *J. Mater. Res.* **2001**, *16*, 1145−1154.
(30) Li, Y. C.; Li, X. H.; Yang, C. H.; Li, Y. F. *J. Phys. Chem. B* **2004**, *108*, 16002−16011.
(31) Li, L. S.; Walda, J.; Manna, L.; Alivisatos, A. P. *Nano Lett.* **2002**, *2*, 557−560.
(32) Sirringhaus, H.; Brown, P. J.; Friend, R. H.; Nielsen, M. M.; Bechgaard, K.; Langeveld-Voss, B. M. W.; Spiering, A. J. H.; Janssen, R. A. J.; Meijer, E. W.; Herwig, P.; de Leeuw, D. M. *Nature* **1999**, *401*, 685−688.

significant differences in the film morphology between films on HMDS and untreated SiO_2 substrates; the improvement in device performance might be related to a decrease in trap states at the ZnO/SiO_2 interface. After spin-coating the films were annealed at 230 °C in forming gas atmosphere to remove the ligand. The device was completed by evaporating Al top source-drain contacts through a shadow mask, which was found to lead to device performance comparable to gold contacts. Aluminum has a work function (4.3 eV) that is matched well to the electron-affinity of ZnO (4.4 eV) and should exhibit only a small barrier for electron injection from Al into the conduction band of ZnO. The device channel length L and width W are $L = 90$ μm and $W = 3$ mm.

The transfer characteristics of the device fabricated from nanorods with different ligands are plotted in Figure 4a. All the devices fabricated from ZnO nanorods with different ligands show n-type behavior. The saturated mobility ($\mu_{sat.}$) is calculated by fitting a straight line to the plot of the square root of I_d vs V_g, according to the expression (for the TFT saturated region): $I_d = (C_i\mu_{sat.}W/2L)(V_g - V_T)^2$ for the case of $V_d > V_g - V_T$, where $C_i = 11.4$ nF/cm^2 is the capacitance of the 300-nm SiO_2 gate dielectric. V_T is the threshold voltage which is typically less than 20 V. The TFT devices with OCTA-ZnO as active layer exhibit significantly higher performance than the films with lower ligand length. OCTA-ZnO films have saturated mobility of 0.1−0.12 cm^2 V^{-1} s^{-1} and an ON/OFF ratio of 10^5−10^6. This is also evident from the output current−voltage characteristics of the device from OCTA-ZnO (Figure 4b). The mobility extracted from the linear region ($V_d = 5$ V) has almost the same values as $\mu_{sat.}$, suggesting a low contact resistance. The mobility value is 5−6 times higher than that of BUTA-ZnO TFT with saturated mobility of 0.015−0.02 cm^2 V^{-1} s^{-1}. Device with HEXA-ZnO show intermediate performance. This improvement of mobility with ligand length is fully consistent with the morphological results described earlier and shows that a high degree of in-plane nanorod alignment and a large domain size are beneficial to transport in the nanorod films. This result also provides evidence that transport in the ZnO films is not limited by residual ligands remaining on the surface of the nanorods after the annealing step since in this case one would expect the films with longer ligands to exhibit poorer performance.

Finally, the device performance of these aligned nanorod films deposited from ligand-modified colloidal nanorods can be enhanced further by subjecting these films to a postdeposition hydrothermal growth step in aqueous zinc solution. As shown in our earlier work, this leads to growth of the nanorods on the substrate, fusing and sintering of the rods and further device improvement.[17] Our initial experiments have shown that after the hydrothermal growth step mobility values of 1.2−1.4 cm^2 V^{-1} s^{-1} and ON/OFF ratio of 10^6−10^7 can be achieved in highly crystalline films grown from OCTA-modified ZnO nanorods. This should be compared to values of 0.4−0.6 cm^2 V^{-1} s^{-1} for BUTA-ZnO subjected to hydrothermal growth. Further optimization of hydrothermal grow conditions may lead to even higher performance.

Conclusions

We have studied the self-assembly of ZnO nanorods with different ligands and have found that small changes in the surface energy of the nanorods induced by the ligands are responsible for large differences in the ability of the nanorods to assemble into highly aligned structures. In spin-coated films long ligands were found to exhibit larger domain size and more pronounced in-plane alignment of the nanorods resulting in significantly better FET device performance than short ligands. We also observed a significant dependence of the preferential orientation of the nanorods on the deposition process. In spin-coated films preferential in-plane alignment of the nanorods was observed, while in drop-cast films with slow evaporation rate nanorods were aligned preferentially normal to the substrate. In films dried slowly between two substrates in-plane alignment was found again with uniaxial nanorod alignment at the edges of the drying film. A model has been proposed to explain this behavior. It is based on the formation of a lyotropic phase on the surface of the drying film. This is favored by using ligands with a low surface tension leading to long nanorod diffusion length on the surface and as a result higher concentrations on the surface which make it easier to reach the critical concentration at which the isotropic solution undergoes the phase transition into the lyotropic phase. The orientation of the nanorods in the dried film can be explained by the direction of liquid flow during the growth. If lateral flow is dominated as in the spin-coating process, the orientation is in plane; if the vertical flow dominates as in drop-casting vertical alignment results. We have also shown that by controlling the self-assembly of the nanorods and promoting in-plane alignment with a large domain size significant improvement of device performance can be achieved. Mobility values of 1.2−1.4 cm^2/V·s in solution processed, in-plane aligned ZnO films subjected to postdeposition hydrothermal growth have been demonstrated. The self-assembly methods presented here are simple, and they can be applied to deposition techniques that are capable of producing uniform films over large areas. Colloidal nanorods are a promising candidate for solution-processed electronic devices that might be able to achieve performance levels which are not accessible with solution-processed organic semiconductors. The techniques for nanorod self-assembly presented here might also be applicable to other materials and optoelectronic devices configuration such as solar cells and light-emitting diodes.

Acknowledgment. We thank Dr. Pietro Cicuta for help with the liquid surface tension measurement. Financial support the Engineering Physical Sciences Research Council and the European Commission is gratefully acknowledged.

Supporting Information Available: Data on the calculation of surface and interface tension and the change of surface potential driving nanoparticle surface segregation. This material is available free of charge via the Internet at http://pubs.acs.org.

JA065242Z